Plant Science 337 (2023) 111890

Contents lists available at ScienceDirect

Plant Science

journal homepage: www.elsevier.com/locate/plantsci

The MPK6-LTF1L1 module regulates lignin biosynthesis in rice through a distinct mechanism from *Populus* LTF1

Ping Zhu [a,1], Yu Zhong [a,1], Laifu Luo [b], Junhui Shen [b], Jiayan Sun [b], Laigeng Li [b,*], Longjun Cheng [a,*], Jinshan Gui [a,*]

[a] State Key Laboratory of Subtropical Silviculture, Zhejiang A&F University, Hangzhou 311300, China
[b] National Key Laboratory of Plant Molecular Genetics, CAS Center for Excellence in Molecular Plant Sciences, Chinese Academy of Sciences, Shanghai 200032, China

ARTICLE INFO

Keywords:
Rice
Populus
Cell wall
Lignin
Transcription factor
Phosphorylation

ABSTRACT

Lignin is a complex polymer that provides structural support and defense to plants. It is synthesized in the secondary cell walls of specialized cells. Through regulates its stability, LTF1 acts as a switch to control lignin biosynthesis in *Populus*, a dicot plant. However, how lignin biosynthesis is regulated in rice, a monocot plant, remains unclear. By employing genetic, cellular, and chemical approaches, we discovered that *LTF1L1*, a rice homolog of *LTF1*, regulates lignin biosynthesis through a distinct mechanism from *Populus* LTF1. Knockout of *LTF1L1* increased lignin synthesis in the sclerenchyma cells of rice stems, while overexpression of *LTF1L1* decreased it. LTF1L1 is phosphorylated by OsMPK6 at Ser^{169}, which did not affect its stability but impaired its ability to repress the expression of lignin biosynthesis genes. This was supported by the non-phosphorylated mutant of LTF1L1 ($LTF1L1^{S169A}$), which displayed a stronger repressive effect on lignin biosynthesis in both rice and *Populus*. Our findings reveal that *LTF1L1* acts as a negative regulator of lignin biosynthesis *via* a distinct mechanism from that of LTF1 in *Populus* and highlight the evolutionary diversity in the regulation of lignin biosynthesis in plants.

1. Introduction

Lignin is a polymer derived from phenylpropanoid that plays a key role in plant secondary cell walls (SCW) by providing mechanical support and facilitating water and nutrient transport for plant growth (Boerjan et al., 2003; Schilmiller et al., 2009; Gui et al., 2011; Cesarino, 2019). Lignin is mainly composed of three monolignols (H, G, and S), which vary in proportions and compositions among different plant species (Boerjan et al., 2003; Dixon and Barros, 2019). For example, gymnosperm lignin is mainly composed of G units with a small amount of H units, while dicot lignin contains mostly G and S units with traces of H units. Monocot lignin, on the other hand, has similar levels of G and S units with a high proportion of H units (Vanholme et al., 2010). Monocot lignin also incorporates a large amount of ferulic acid, tricin, hydroxycinnamates, and ρ-coumaric acid, which form unique lignin structures in specific cell types, such as sclerenchyma cells (Vanholme et al., 2010; Verma and Dwivedi, 2014; Lan et al., 2015; Xie et al., 2018). Lignin biosynthesis is regulated by developmental and environmental signals. Although the regulation of lignin biosynthesis in dicots has been widely studied, less is known about the regulation of lignin biosynthesis in monocots, as the two types of plants have differing secondary cell wall formation.

Lignin biosynthesis is controlled by a hierarchical network of transcriptional regulators, including activators and repressors (Zhong et al., 2011; Hirano et al., 2013a; Luo and Li, 2022). Some of these transcription factors have similar functions in monocots and dicots, but others have different regulatory mechanisms. For instance, SND1 is an activator that regulates itself by binding to its own promoter and is repressed by its downstream MYB factors in Arabidopsis (Wang et al., 2011). However, the feedback regulation of OsSWN1 and OsSWN2, two rice orthologs of SND1, is mediated by the alternatively spliced form of OsSWN2 (Yoshida et al., 2013). MYB58/63 are lignin-specific regulators in Arabidopsis and other dicot plants (Zhou et al., 2009). However, overexpressing OsMYB58/63 in rice increased both lignin and cellulose biosynthesis (Noda et al., 2015). Furthermore, *MYB103* is required for syringyl lignin biosynthesis in Arabidopsis, whereas *MYB103L*, a rice

* Corresponding authors.
E-mail addresses: lgli@cemps.ac.cn (L. Li), ljcheng@zju.edu.cn (L. Cheng), jsgui@zafu.edu.cn (J. Gui).
[1] These authors equally contributed to the study.

https://doi.org/10.1016/j.plantsci.2023.111890
Received 6 September 2023; Received in revised form 22 September 2023; Accepted 4 October 2023
Available online 9 October 2023

MYB103 ortholog, regulates cellulose biosynthesis (Ohman et al., 2013; Yang et al., 2014; Ye et al., 2015; Wu et al., 2021). There are also transcriptional repressors such as MYB4 and other subgroup 4 R2R3 MYB factors that suppress lignin biosynthesis. MYB4 has an ERF-associated amphiphilic repression (EAR) motif (pdLNLD/LxiG/S) that confers its transcriptional repression activity (Ma and Constabel, 2019). The Arabidopsis MYB4 negatively regulates lignin biosynthesis by suppressing the expression of genes involved in the phenylpropanoid pathway (Zhou et al., 2017; Lin et al., 2022). Similarly, EgMYB1 in *Eucalyptus gunnii*, ZmMYB31 and ZmMYB42 in maize, OsMYB102 and OsMYB108 in rice repress lignin biosynthesis (Vélez-Bermúdez et al., 2015; Miyamoto et al., 2019; Lin et al., 2022). However, the exact mechanisms that regulate the subgroup 4 R2R3-MYB factors for lignin biosynthesis are not fully understood.

Protein phosphorylation is a post-translational modification that can change protein function, stability, localization, and interaction (Cohen, 2000). Mitogen-activated protein kinase (MAPK) mediated protein phosphorylation is crucial to plant growth and development, immunity, and abiotic stress tolerance (Zhao et al., 2017; Sun et al., 2018; Liu et al., 2022). MPK3/MPK6 regulates lignin biosynthesis by phosphorylating transcription factors that control lignin biosynthesis genes (Sulis and Wang, 2020). For example, LTF1, a transcription repressor of lignin biosynthesis, is phosphorylated by PdMPK6, which leads to its degradation and activation of lignin biosynthesis genes (Gui et al., 2019). OsMAPK10 mediated RLM1 phosphorylation enhances RLM1 binds to the promoter of OsCAD2 (Chen et al., 2022). NST1 can be phosphorylated by SnRK2 to regulate ABA-mediated lignin biosynthesis (Liu et al., 2021). Moreover, enzymes in the lignin biosynthetic pathway are also regulated by phosphorylation. For example, PAL can be phosphorylated by calmodulin-like domain protein kinase (CDPK) family proteins, which alters its stability (Allwood et al., 1999), and PtrAldOMT2 phosphorylation controls syringyl monolignol biosynthesis (Wang et al., 2015).

In this study, we discovered that LTF1L1, an R2R3 MYB transcription factor in rice, is phosphorylated by OsMPK6 through direct interaction, and that LTF1L1 switches its transcriptional repression activity depending on its phosphorylation status to regulate lignin biosynthesis.

2. Materials and methods

2.1. Plant materials and growing conditions

Oryza japonica variety Zhonghua 11 (ZH11) was used as a wild-type control and as a source material for generating mutants and transgenic rice plants. We compared ZH11 with the OsMPK6 mutant *dsg1*, which has the same genetic background, and with the *LTF1L1* mutants' *ltf1l1* and *ltf1l1 ltf1l2*, and the overexpressing transgenic rice *LTF1L1-OE* and *LTF1L1^{A}-OE*. We grew rice plants either in a paddy field under natural conditions or in a growth chamber with a photon flux density of 200 ~ 250 μmol m^{-2} s^{-1} and a temperature cycle of 28 ℃/22 ℃ (day/night) for 14 h/10 hr. For *Populus* experiments, we used *Populus deltoides* × *Populus euramericanan* cv. "Nanlin895″ to generate *LTF1L1* and *LTF1L1^{A}* transgenic plants. We grew *Populus* plants in a phytotron with 60% relative humidity, 12 h photoperiod at 24 ℃ and light intensity of 100 ~ 200 μmol m^{-2} s^{-1}.

2.2. Generation of transgenic plants

LTF1L1 CRISPR/Cas9 vectors were constructed by cloning sgRNA expression cassettes with gene-specific target sequences of *LTF1L1* and *LTF1L2* into a *pYLCRISPR/Cas9-H* plasmid according to (Ma et al., 2015). Full-length CDS of *LTF1L1* and its non-phosphorylated variant *LTF1L1^{S169A}* (designated as *LTF1L1^{A}*) were cloned into *pUN1301–3Flag* vector for rice and *pCAMBIA2300:^{35}S–^{3}Flag* vector for *Populus* to generate overexpression transgenic lines. We confirmed the vectors by sequencing and transferred them into *Agrobacterium tumefaciens* strain EHA105 for rice and GV3101 for *Populus*. The transgenic plants were regenerated *via* as described previously (Hiei et al., 1994; Li et al., 2003). The primers used are listed in Table S2.

2.3. Histochemical staining

Cross sections of the 3-month-old rice culms and 2-month-old Populus internodes stained with Phloroglucinol-HCl [1% phloroglucinol (w/v) in 12% HCl] was performed as described (Gui et al., 2011). The stained sections were immediately observed with a microscope (Olympus BX53).

2.4. Cell-wall composition analysis

Rice culms and *Populus* xylem tissues were harvested and dried at 55 ℃. The dried samples were ground to powder by ball milling to prepare cell wall residues. The cell wall residues were treated with 10 μl of amylase (50 μg/ml, from *Bacillus species*; Sigma-Aldrich) and 5 μl of pullulanase (18.7 units, from *Bacillus acidopullulyticus*; Sigma-Aldrich) to remove starch. Lignin and crystalline cellulose content were analyzed as previously described (Gui et al., 2019). Monosaccharide compositions of samples were analyzed as previously described (Pettolino et al., 2012).

2.5. Protein interaction assays

For the BiFC analysis, the coding sequences of *LTF1L1* and *OsMPK6* were cloned into the *pCAMBIA1300–35S-YN* and *pCAMBIA1300–35S-YC* vectors respectively. The verified plasmids were co-transformed into *GV3101* and used for *N. benthamiana* leaf cells transformation, individually or combined, for BiFC assay as previously described (Gui et al., 2016).

For the co-immunoprecipitation (Co-IP) and western blot assay, OsMPK6 with Flag tag and Myc-tagged *LTF1L1* were overexpressed in tobacco. The proteins were extracted from tobacco materials after 2 days of incubation. Anti-Flag antibody-coupled agarose beads (Sigma) were used to co-precipitate LTF1L1 and OsMPK6 and western blot assay was performed.

2.6. Subcellular localization assay

The full length *LTF1L1* coding sequence was cloned into the *pCAMBIA1300–35S-mCherry* vector and transformed into GV3101 for transient transformation of tobacco leaves as described (Gui et al., 2016). After 48 h of incubation, the transformed leaf cells were stained with DNA-binding dye 4′, 6 diamidino-2phenylindole (DAPI). The mCherry and DAPI fluorescence was examined using a confocal microscope (FV1000; Olympus).

2.7. Yeast one-hybrid assays

To test LTF1L1 binding to the *Os4CL3* promoter, the coding sequence of *LTF1L1* was fused with *GAL4-AD* to construct the *pPC86-LTF1L1* plasmid. The *Os4CL3* promoter fragment (199–412 bp upstream of the initiation codon ATG) and *PdCESA8* promoter fragment (188–600 bp upstream of the initiation codon ATG) were cloned into *p178* vector producing the *Os4CL3-lacZ* and *PdCESA8-lacZ* reporter plasmid, respectively. The two vectors were co-transformed into the yeast *Saccharomyces cerevisiae* strain EGY48 to perform yeast one hybrid assay according to the manufacturer's protocol using O-nitrophenyl β-D-galactopyranoside as a substrate (Clontech).

2.8. Electrophoretic mobility shift assay

The full length coding sequence of *LTF1L1* was cloned into the *pET28a* (+) vector and fused with a His6 tag at the C terminus (Novagen). LTF1L1-His protein was expressed in the *E. coli* BL21 (DE3) strain

(Invitrogen) and purified using nickel-nitrilotriacetic acid resin (Qiagen). Fragments of the Cy5-labeled *Os4CL3* promoter were produced by PCR amplification using Cy5-labeled fluorescent primers. EMSA was performed as previously described (Gui et al., 2016).

2.9. Transcriptional activity assay by the dual-luciferase reporter assay system

Arabidopsis protoplasts were prepared as described (Yoo et al., 2007). We cloned the 1.5 kb *Os4CL3* promoter and the 35 S mini promoter into *pGreen II 0800-LUC* as the reporter vector. We also cloned the *LTF1L1* coding sequence and the Ser^{169} site changed to Alanine version of *LTF1L1* into *pCAMBIA2300:35 S* as the effector vectors. The effector and reporter plasmids were co-transfected into protoplasts and cultured for 12–16 h at 25 ℃ in the darkness. We measured the LUC activities using the dual-Luciferase reporter assay system (Promega, USA). The firefly LUC to the renilla LUC (REN) ratio represents the relative LUC activity.

2.10. Gene expression analysis

Total RNA was extracted from rice seedlings (2 weeks old) and *Populus* internodes (2 months old) using a total RNA extraction kit (Omega). Each sample, 2 μg of total RNA was reverse-transcribed into first-strand complementary DNA (cDNA) using a TransScript first-strand cDNA synthesis supermix (Transgen). Gene expression analysis was performed with an ABI QuantStudio 3 real-time PCR system (Thermofisher) and PerfectStart green qPCR supermix (Transgen). The gene expression data were normalized using the rice Actin1 gene (Os03g0718100). The primers used are listed in Table S2.

2.11. In-vitro phosphorylation assays

The full length coding sequences of *LTF1L1*, $LTF1L1^{A}$ (S169A), and $OsMKK4^{DD}$ (constitutively active *OsMKK4*) were cloned into *pET28a* (+) (Novagen) with a His6 tag at the C terminus. *OsMPK6* was cloned into *pGEX-6p-1* vector (GE Healthcare) with a glutathione S-transferase tag. These recombinant proteins were purified and performed *in-vitro* phosphorylation assay as previously described (Gui et al., 2019). Protein phosphorylation was analyzed by SDS-PAGE, and obtained images using a Typhoon FLA 9000 phosphor imager (Amersham).

3. Results

3.1. LTF1L1 knockout enhances lignin deposition in sclerenchyma cells of rice

Previously, we identified that *LTF1*, a MYB transcription factor, regulates lignin biosynthesis through PdMPK6-mediated protein stability in *Populus* (Gui et al., 2019). To investigate the evolutionary conservation of *LTF1* in monocots, we searched the rice genome for genes homologous to *LTF1*. We identified two genes (*LOC_Os08g43550* and *LOC_Os09g36730*) that share 58.6% and 66.4% sequence similarity with *LTF1*, respectively. We named them *LTF1L1* and *LTF1L2* (Fig. S1). To examine the genetic function of *LTF1L1* in rice, we used the CRISPR/-Cas9 genome editing technique to generate single (*ltf1l1*) and double (*ltf1l1 ltf1l2*) mutants. We confirmed the mutations by PCR and sequencing (Fig. S2). Compared with the wild-type, both the *ltf1l1* and the *ltf1l1 ltf1l2* mutants had compact plant architecture with extremely erect tillers, leaf blades, and panicles, indicating that *LTF1L1* affects the mechanical support for the upright growth of rice plants (Fig. 1a). We also observed that both the mutants had stronger lignin staining in the sclerenchyma cells than the wild-type (Fig. 1b). Chemical composition of the cell wall tests in culms revealed that the *ltf1l1* and the *ltf1l1 ltf1l2* mutants had about 17% and 20% more lignin content, respectively (Fig. 1c) but no significant difference in crystalline cellulose and hemicellulose monosaccharide content (Fig. 1d, Fig. S3). Furthermore, the transcript levels of key lignin biosynthesis genes (*PAL1*, *C4H1*, *4CL3*, *COMT1*, and *CAD1*) were markedly higher in the mutants than in the wild-type, while the transcript levels of cellulose biosynthesis genes

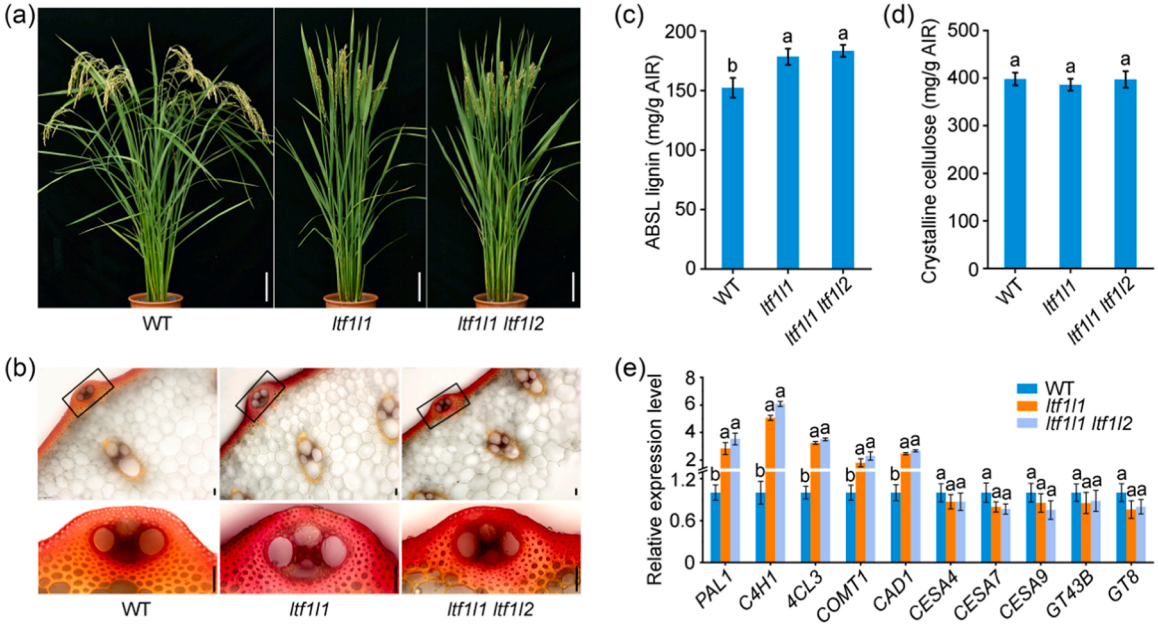

Fig. 1. Knockout of *LTF1L1* increased lignin deposition in sclerenchyma cells. (a) Morphology of WT, *ltf1l1*, and *ltf1l1 ltf1l2* rice plants at the grain-filling stage. *ltf1l1 ltf1l2* is a double mutant of *LTF1L1* and *LTF1L2*. Scale bar, 10 cm. **(b)** Cross-sections of the third internode from WT, *ltf1l1*, and *ltf1l1 ltf1l2* stained with phloroglucinol-HCl (upper panel). The lower panel shows close-up images of the sclerenchyma cells (black box in the upper panel). Scale bar, 50 μm. **(c, d)** Lignin content (c) and crystalline cellulose content (d) in the culms of WT, *ltf1l1*, and *ltf1l1 ltf1l2* rice plants in mature stems. Results are means ± SE of three replicate determinations. ABSL, acetyl bromide-soluble lignin. **(e)** Expression of genes involved in secondary cell wall biosynthesis in 2-week-old seedlings. Gene expression was determined by qRT-PCR analysis. Results are means ± SE of three biological repeats. In (c) to (e), different lowercase letters indicate significant differences at $P < 0.01$ by ANOVA.

(*CESA4*, *CESA7*, and *CESA9*) and hemicellulose biosynthesis genes (*GT43B* and *GT8*) did not change significantly between the mutants and the wild-type (Fig. 1e). These results suggested that *LTF1L1* acts as a negative regulator of lignin biosynthesis in sclerenchyma cells.

3.2. Phosphorylation modulates LTF1L1 function in lignin biosynthesis in rice

To investigate how *LTF1L1* regulates lignin biosynthesis, we generated transgenic plants overexpressing *LTF1L1* (*L1OE*) driven by the CaMV 35 S promoter. We obtained 21 independent *L1OE* transgenic lines, which have similar morphologies. We selected two representative transgenic lines of the *LTF1L1*-overexpression *L1OE 6* and *L1OE 8* for more detailed characterization. Compared with the wild-type, *L1OE* transgenics had slightly shorter plant height (Fig. 2a, Table S1). To examine if *L1OE* affects lignin biosynthesis, we performed histochemical staining and chemical tests. The *L1OE* transgenics exhibited lighter red staining in sclerenchyma cells that appeared red in the wild-type, suggesting that *L1OE* has less lignin than WT (Fig. 2b). Chemical tests of culms showed that lignin content was reduced by 6~11% in the *L1OE* transgenics compared to the wild-type (Fig. 2c). However, crystalline cellulose content did not differ significantly between *L1OE* and WT (Fig. 2d).

LTF1L1 transcript levels in *L1OE 6* and *L1OE 8* lines were about 11-fold and 68-fold higher than in WT, respectively (Fig. 2e). However, the growth phenotypes and lignin content of the two lines were similar (Fig. 2a-c). To further examine if LTF1L1 protein abundance was responsible for the phenotypes and lignin content between *L1OE 6* and *L1OE 8* lines, we measured protein abundance of LTF1L1 by using Western blot analysis. LTF1L1 protein abundance in *L1OE 8* was about 5-fold higher than in *L1OE 6* (Fig. 2f), indicating that the LTF1L1 protein is stable and consistent with its transcript levels. These results suggest that LTF1L1 may regulate lignin biosynthesis through post-translational modification.

To test this hypothesis, we performed immunoprecipitation and LC-MS/MS analysis of nuclear proteins from *L1OE 8* plants and identified two phosphorylation sites on LTF1L1, Thr^{145} and Ser^{169} (Fig. 2g-h). Since the *Populus* homolog of LTF1L1, LTF1, is phosphorylated by PdMPK6 in *Populus* (Gui et al., 2019), we further examined whether OsMPK6 could phosphorylate LTF1L1 at these sites in rice.

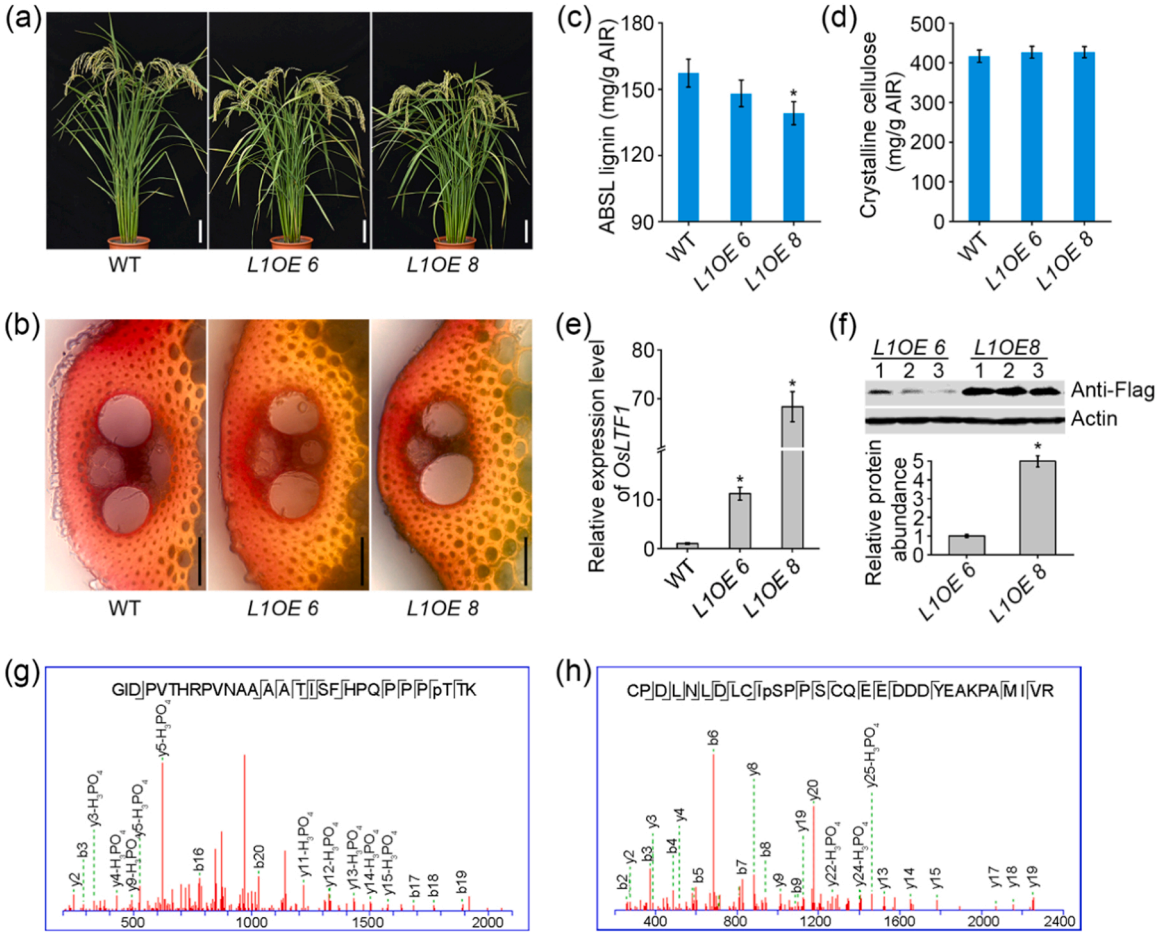

Fig. 2. LTF1L1 protein abundance showed no significant correlation with lignin biosynthesis in sclerenchyma cells of rice. (a) Morphology of the WT and *LTF1L1* overexpressing (*L1OE*) transgenic lines at the grain-filling stage. Scale bar, 10 cm. **(b)** Cross-sections of the third internode from WT and *L1OE* rice plants stained for lignin with phloroglucinol-HCl. Scale bar, 50 μm. **(c, d)** Quantification of lignin content (c) and crystalline cellulose content (d) in the culms of WT and *L1OE* rice plants in mature stems. Results are means ± SE of three replicate determinations. **(e)** Relative expression level of *LTF1L1* in WT and *L1OE* at 2-week-old seedlings measured by qRT-PCR. Results are means ± SE of three biological repeats. **(f)** Protein abundance of LTF1L1 in *L1OE 6* and *L1OE 8* at 2-week-old seedlings was determined by immunoblotting assay using anti-Flag antibody (upper panel).The signal density was quantified based on the three biological replicates (lower panel). The relative protein abundance in *LTF1L1* overexpressing line *L1OE6* was set as 1. In (c), (e), and (f), single asterisk indicates that the difference between the wild-type and *L1OE* transgenics is statistically significant at $P < 0.01$ by t-test. (g, h) Identification of LTF1L1 phosphorylation sites at Thr145 and Ser169 residues in *planta* by LC-MS/MS analysis. LTF1L1–3Flag protein was immunoprecipitated by anti-Flag agarose beads from the 2-week-old rice seedlings and subjected to LC-MS/MS analysis. Two peptides containing phosphorylated residues were identified: GIDPVTHRPVNAAAATISFHPQPPP(pT)TK (g) and CPDLNLDLCI(pS)PPSCQEEDD-DYEAKPAMIVR (h), corresponding to Thr145 (g) and Ser169 (h) in LTF1L1. The phosphorylated residues are marked as pT and pS, respectively.

3.3. LTF1L1 interacts with and is phosphorylated by OsMPK6

To verify the interaction between LTF1L1 and OsMPK6, we performed bimolecular fluorescence complementation (BiFC) and co-immunoprecipitation (Co-IP) assay. In BiFC, we co-expressed *LTF1L1* tagged with the C-terminal half of *YFP* (*LTF1L1-YC*) and *OsMPK6* fused with the N-terminal half of yellow fluorescent protein (YFP) (*OsMPK6-YN*) in tobacco leaf epidermal cells and observed a strong fluorescent signal in the nucleus (Fig. 3a). No fluorescence signal was detected when *PdMPK6-YN* and *YC* were co-expressed, or *LTF1L1-YC* and *YN* were co-expressed (Fig. 3a). In addition, the interaction between LTF1L1 and OsMPK6 was independently verified by Co-IP in tobacco leaves. LTF1L1 co-immunoprecipitated with OsMPK6 when both Myc-tagged *LTF1L1* (*LTF1L1-Myc*) and Flag-tagged *OsMPK6* (*OsMPK6-Flag*) were co-expressed, but not when *OsMPK6-Flag* was expressed alone, indicating a direct interaction between LTF1L1 and OsMPK6 (Fig. 3b).

To test if OsMPK6 directly phosphorylates LTF1L1 at Thr^{145} and/or Ser^{169}, we produced recombinant His-tagged LTF1L1, $LTF1L1^{T145A}$, $LTF1L1^{S169A}$, $LTF1L1^{T145AS169A}$, OsMPK6, and $OsMKK4^{DD}$ (constitutively active OsMKK4) (Kishi-Kaboshi et al., 2010) in *E. coli* (Fig. S4). We performed *in vitro* phosphorylation assays and found that LTF1L1 was phosphorylated by OsMPK6 in the presence of $OsMKK4^{DD}$ (Fig. 3c), indicating that the activated OsMPK6 can phosphorylate LTF1L1. When we mutated Thr^{145} or Ser^{169} in LTF1L1 to alanine, we found that Thr^{145} had no effect on the phosphorylation level of LTF1L1, but Ser^{169} was essential for the phosphorylation by OsMPK6 (Fig. 3c). These results indicated that Ser^{169}, but not Thr^{145}, is the major site in LTF1L1 phosphorylated by OsMPK6.

3.4. OsMPK6 modulates lignin deposition and secondary cell wall formation in rice

To examine whether *OsMPK6* is involved in lignin biosynthesis, we stained the cross-sections of the *OsMPK6* mutant *dsg1* (Liu et al., 2015) and wild-type plants for lignin with phloroglucinol-HCl. The *dsg1* mutant exhibited weaker red staining in vascular bundles and sclerenchyma cells than the wild-type control, indicating lower lignin content in the *dsg1* mutant (Fig. S5a). We also measured the SCW composition and found that the *dsg1* mutant had about 22% less lignin content and 9% less crystalline cellulose content than the control (Fig. S5b,c). In addition, the expression of key lignin biosynthesis genes (*PAL1*, *C3H1*, *4CL3*, *COMT1*, and *CAD1*) and cellulose synthase genes (*CESA4*, *CESA7*, and *CESA9*) was significantly down-regulated in the *dsg1* mutant compared to the wild type, while the transcript levels of genes related to hemicellulose biosynthesis (*GT43B* and *GT8*) did not change significantly (Fig. S5d). These results suggested that *OsMPK6* regulates secondary cell wall formation by controlling both lignin and cellulose biosynthesis in vascular bundles and sclerenchyma cells in rice.

3.5. $LTF1L1^{S169A}$ mutation strongly inhibits lignin biosynthesis in rice sclerenchyma cells

To investigate if the phosphorylation of LTF1L1 at Ser^{169} by OsMPK6 affects its ability to repress lignin biosynthesis, we generated a non-

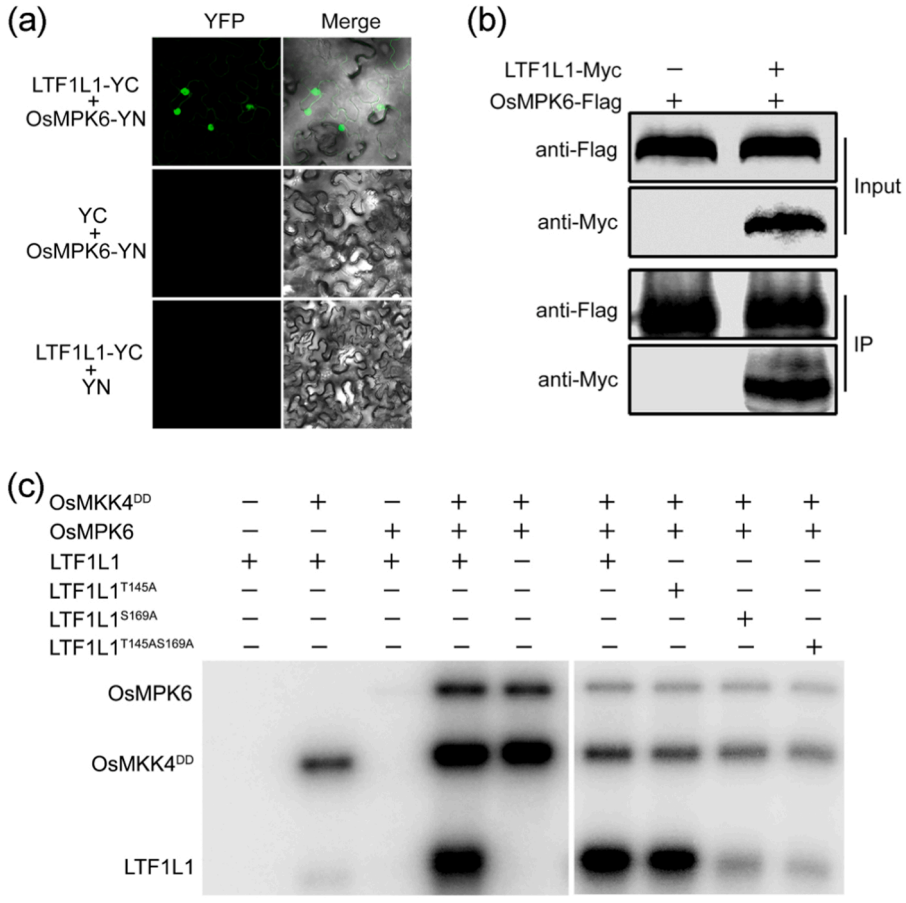

Fig. 3. LTF1L1 interacts with and is phosphorylated by OsMPK6. (a, b) Interaction between LTF1L1 and OsMPK6 was confirmed by bimolecular fluorescence complementation (BiFC) assays (a) and co-immunoprecipitation (Co-IP) analyses (b) **(c)** In vitro phosphorylation assay of LTF1L1 and its mutants with altered phosphorylation sites. $LTF1L1^{T145A}$, $LTF1L1^{S169A}$, and $LTF1L1^{T145AS169A}$ have threonine 145, serine 169, or both residues replaced by alanine, respectively. Recombinant $OsMKK4^{DD}$, a constitutively active form of OsMKK4, was used to activate OsMPK6. LTF1L1 or its mutants were incubated with or without OsMPK6 and $OsMKK4^{DD}$ at 30 °C for 1 h. After separation on an SDS-PAGE gel, images were obtained using a phosphor imager.

phosphorylated version of LTF1L1, LTF1L1^{S169A} (LTF1L1^{A}), and overexpressed it in rice plants (*L1^{A}OE*). We obtained 32 independent *L1^{A}OE* transgenic lines, most of which the *L1^{A}OE* lines showed dramatic morphological changes compared with the wild-type. Two representative transgenic lines (*L1^{A}OE 2* and *L1^{A}OE 3*) were selected for further characterization. Compared with the wild-type, *L1^{A}OE* transgenics exhibited loose plant architecture with soft culms, shorter plant height, shorter internodes, and droopy leaves (Fig. 4a-c, Table S1). These phenotypic changes suggested that *L1^{A}OE* plants had reduced mechanical strength of culms and leaves, which might be related to altered cell wall formation and lignin biosynthesis. Therefore, we performed histochemical staining followed by chemical tests and gene expression analysis to further examine SCW formation and lignin deposition. The *L1^{A}OE* transgenics displayed visibly lighter yellow color in sclerenchyma cells that appeared red in the wild-type (Fig. 4d). This suggests that *L1^{A}OE* has less lignin than the wild-type. Chemical tests of culms showed that lignin content was reduced by 23~27% in the *L1^{A}OE* transgenics compared to the wild-type (Fig. 4e). However, crystalline cellulose content did not change significantly between the transgenics and the wild-type (Fig. 4f). These results indicated that LTF1L1^{A} specifically suppressed lignin biosynthesis without affecting cellulose biosynthesis in SCWs.

LTF1L1 transcript levels varied greatly among different lines. Among them, the *L1OE 6* and *L1^{A}OE 2* transgenic lines had similar transcript levels of *LTF1L1*, which were about 10-fold higher than in the WT (Fig. 4g). However, the growth phenotypes and lignin content of the two types of transgenics exhibited dramatically different (Fig. 2a-c, Fig. 4a-c). To investigate whether the differences in growth were caused by the abundance of LTF1L1 protein, we performed Western blot analysis to measure the protein level of LTF1L1. Surprisingly, we found that the *L1^{A}OE* transgenic lines *L1^{A}OE 2*, *L1^{A}OE 3* and the *L1OE* transgenic line *L1OE 6* had similar level of LTF1L1 protein, while the *L1OE* transgenic line *L1OE 8* had a much higher level of LTF1L1 protein (Fig. 4h). These results indicated that the phosphorylation of LTF1L1 by OsMPK6 at Ser^{169} did not affect its protein stability in rice (Fig. 4g,h). This was different to the previous finding that phosphorylation affects LTF1 protein stability in *Populus* (Gui et al., 2019). These findings suggest that MPK6-mediated phosphorylation of rice LTF1L1 and *Populus* LTF1 may have different regulatory mechanisms for controlling lignin biosynthesis.

We examined the transcript levels of five lignin biosynthesis genes (*PAL1*, *C4H1*, *4CL3*, *COMT1*, and *CAD1*) in *L1OE* and *L1^{A}OE* transgenic

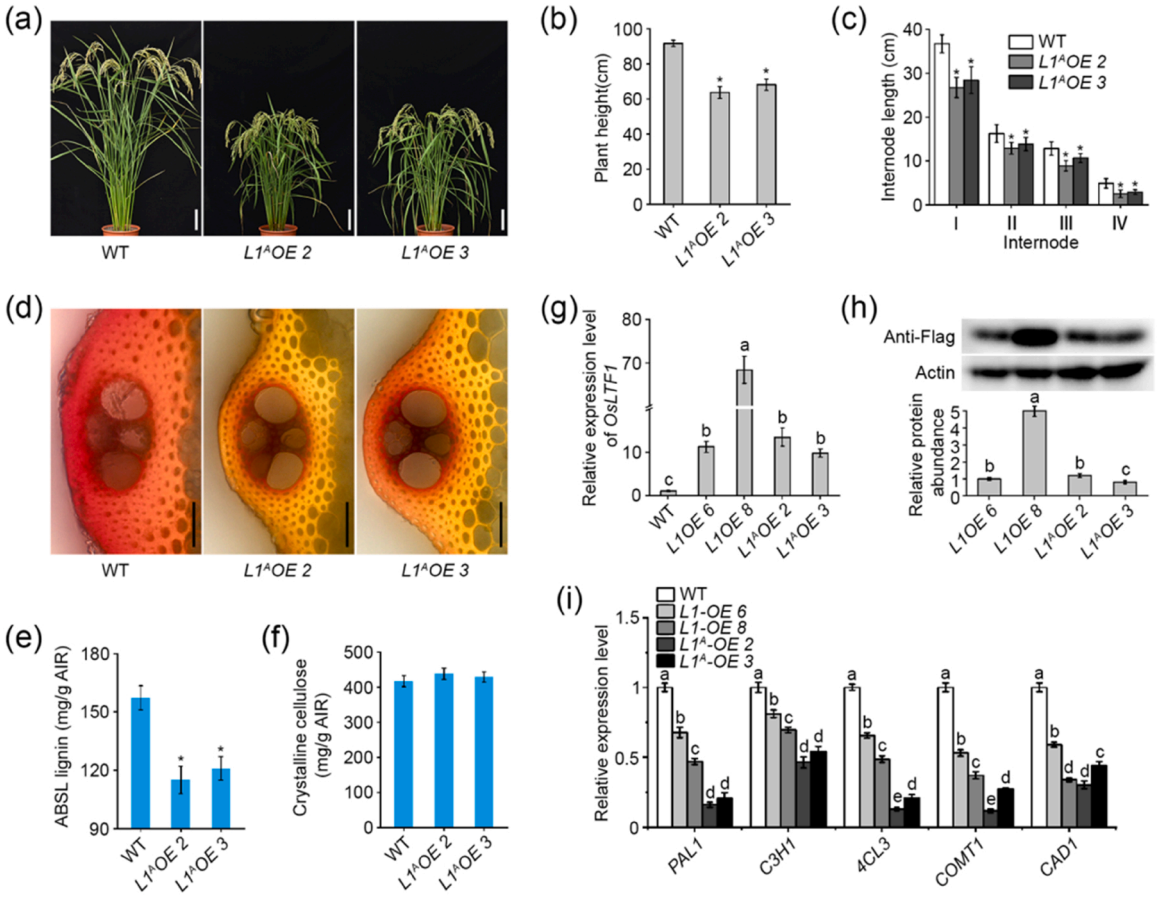

Fig. 4. Expression of *LTF1L1^{S169A}* strongly suppressed lignin biosynthesis in sclerenchyma cells. (a) Morphology of the WT and *LTF1L1^{S169A}* overexpressing (*L1^{A}OE*) transgenic lines at the grain-filling stage. *LTF1L1^{S169A}* is a mutant form of *LTF1L1* with serine 169 replaced by alanine. Scale bar, 10 cm. **(b, c)** The plant height (b), and internode length (c) of WT and *L1^{A}OE* plants were measured and compared. Results are means ± SE of fifteen biological replicates. **(d)** Cross-sections of the third internode from WT and *L1^{A}OE* rice plants stained with phloroglucinol-HCl. Scale bar, 50 μm. **(e, f)** Lignin content (e) and crystalline cellulose content (f) in the culms of WT and *L1^{A}OE* rice plants in mature stems. Results are means ± SE of three replicate determinations. **(g)** Relative expression level of *LTF1L1* in WT, *L1OE*, and *L1^{A}OE* transgenic lines at 2-week-old seedlings. Results are means ± SE of three biological replicates. **(h)** Protein abundance of LTF1L1 in WT, *L1OE*, and *L1^{A}OE* transgenic lines at 2-week-old seedlings was determined by immunoblotting assay (upper panel).The signal density was quantified based on the three biological replicates (lower panel). The relative protein abundance in *LTF1L1* overexpressing line *L1OE6* was set as 1. **(i)** Expression of lignin biosynthesis genes in WT, *L1OE*, and *L1^{A}OE* transgenic lines at 2-week-old seedlings. Results are means ± SE of three biological replicates. In (b), (c), (e), and (i), single asterisk indicates that the difference between the wild-type and *L1^{A}OE* transgenics is statistically significant at $P < 0.01$ by t-test. In (g) and (h), different lowercase letters indicate significant differences at $P < 0.01$ by ANOVA.

plants. Both *L1OE* and *L1^{A}OE* had lower expression of these genes than the wild type, but *L1^{A}OE* had much lower expression than *L1OE* (Fig. 4i). This was unexpected because *L1OE* had more *LTF1L1* transcript and protein than *L1^{A}OE*. We inferred that the phosphorylation status of the LTF1L1 was critical for controlling lignin biosynthesis.

3.6. *LTF1L1 phosphorylation at Ser^{169} impairs its transcriptional repressor activity*

To investigate how LTF1L1 phosphorylation affects lignin biosynthesis, we performed a series of experiments to examine its subcellular localization, DNA-binding ability, and transcriptional repressor activity. The results showed that both LTF1L1-mCherry and LTF1L1^{A}-mCherry signal overlapped with the nuclear marker DAPI, suggesting that LTF1L1 was localized in the nucleus and phosphorylation did not change its localization (Fig. 5a). We then tested whether LTF1L1 directly binds to the promoter of *4CL3*, a key lignin biosynthesis gene (Gui et al., 2011), because the expression of *4CL3* is induced in the *ltf1l1* mutant and suppressed by LTF1L1 overexpression (Fig. 1e, Fig. 4i). Yeast one-hybrid assay showed that LTF1L1 bound to the *4CL3* promoter but not to the *CESA9* promoter (Fig. 5b). This result was confirmed by electrophoretic mobility shift assay (EMSA) (Fig. 5c). We incubated two proteins, His-tagged LTF1L1 and His-tagged LTF1L1^{A}, with Cy5-labeled probe of the *4CL3* promoter fragment. The probe showed a clear and comparable band shift for both proteins, while the free probe did not show any shift (Fig. 5c), indicating that LTF1L1 and LTF1L1^{A} bind directly to the *4CL3*

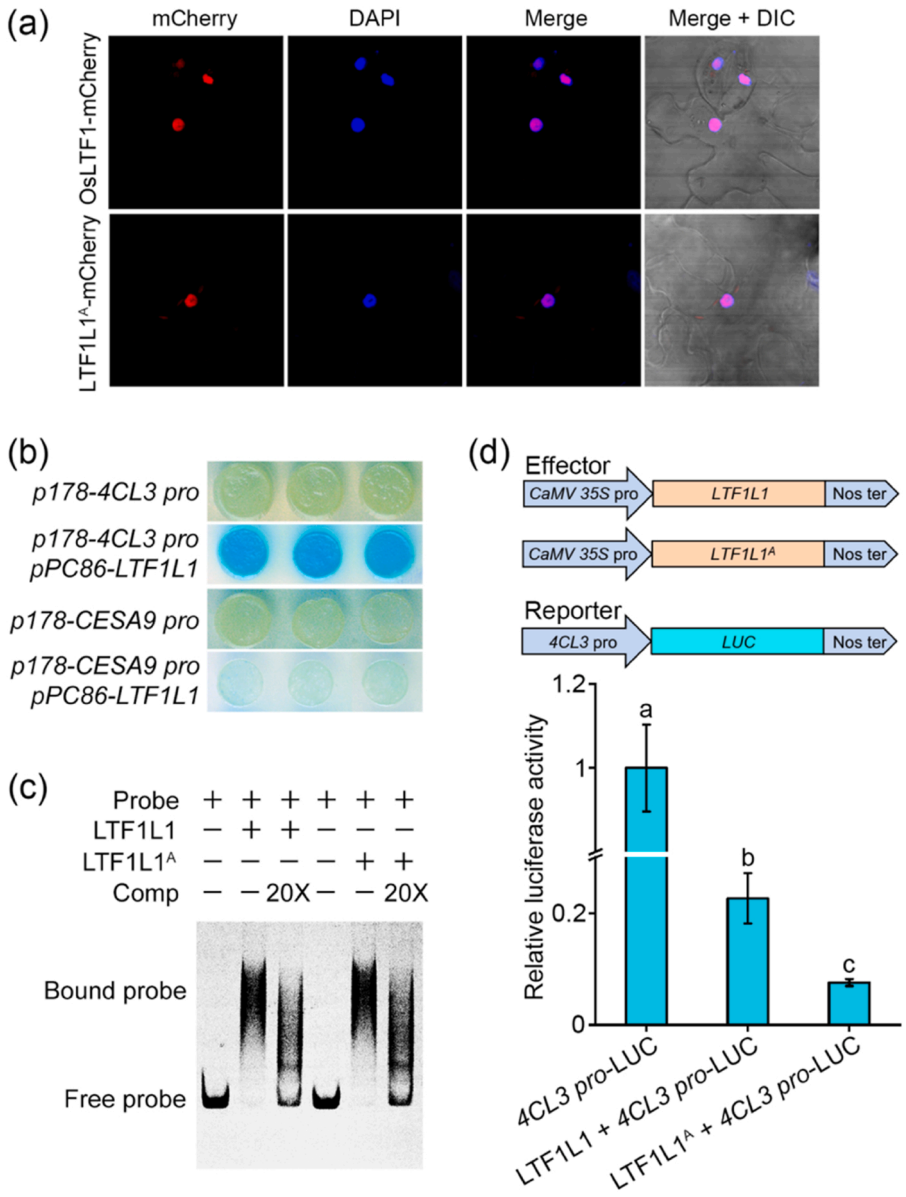

Fig. 5. Non-phosphorylated LTF1L1 (LTF1L1^{S169A}) enhances LTF1L1 transcriptional repressor activity. (a) Subcellular localization of LTF1L1 and LTF1L1^{S169A} in nuclei. LTF1L1 and LTF1L1^{S169A} were fused with mCherry, showing co-localization with the 4′, 6-diamidino-2-phenylindole (DAPI) stained nucleus in tobacco epidermal cells. **(b)** LTF1L1 binding to rice *4CL3* promoter was examined by yeast one-hybrid analysis. The yeast strain EGY48 was transformed with *pPC86-LTF1L1* as effector plasmid and *p178–4CL3*Pro as reporter plasmid. The blue color on X-gal medium indicates LTF1L1 binds to *4CL3* promoter. **(c)** LTF1L1 binding to rice *4CL3* promoter was verified by electrophoretic mobility shift assay (EMSA). The Cy5-labeled DNA probe containing the LTF1L1 binding site in the *4CL3* promoter was incubated with recombinant LTF1L1 protein. The shifted bands indicated the formation of protein-DNA complexes. **(d)** Activity of LTF1L1 and LTF1L1^{A} in regulating *4CL3* expression by dual-luciferase reporter assay. Effector and reporter vectors were shown in the upper panel. The relative luciferase activity for promoter of *4CL3* fused with 35 S mini promoter was calculated as firefly luciferase / renilla luciferase ratio. Results are means ± SE of five replicates. The luciferase activity in the *4CL3pro*-LUC alone was set as 1. Different letters indicate significant differences at $P < 0.01$ by ANOVA.

promoter and the phosphorylation of LTF1L1 at Ser^{169} does not affect its DNA-binding ability.

We next examined how LTF1L1 phosphorylation affects *4CL3* expression using a dual-luciferase reporter system. We generated a reporter vector with a 1.5 kb *4CL3* promoter and a 35 S mini promoter driven *LUC* expression, and an effector vector with a 35 S promoter driven *LTF1L1* or *LTF1L1^{A}* expression (Fig. 5d). We co-transformed these vectors into Arabidopsis protoplasts and measured LUC activity as an indicator of *4CL3* expression. We found that LTF1L1 significantly reduced LUC activity compared to the empty vector control (Fig. 5d), indicating that it repressed *4CL3* transcription. Moreover, this effect was stronger when we used LTF1L1^{A} instead of LTF1L1 (Fig. 5d), suggesting that phosphorylation impairs LTF1L1′s transcriptional repressor activity. These results indicated that LTF1L1 phosphorylation modulates *4CL3* expression and lignin biosynthesis in rice.

3.7. *LTF1L1^{S169A} mutation enhances its repression of lignin biosynthesis genes in Populus, independent of its stability*

LTF1L1 and LTF1 are homologous proteins that inhibit lignin biosynthesis in rice and *Populus*, respectively. However, they have different regulatory mechanisms. In *Populus*, LTF1 is phosphorylated by PdMPK6, which triggers its degradation and releases its inhibition on lignin biosynthesis (Gui et al., 2019). In rice, LTF1L1 is phosphorylated by OsMPK6, which impairs its repressive activity but not protein stability. To test if *LTF1L1* has a similar effect in *Populus* as in rice, we overexpressed *LTF1L1* and *LTF1L1^{A}* (non-phosphorylation form) genes under the CaMV 35 S promoter in *Populus* and generated transgenic lines (*L1OE* and *L1^{A}OE*). We obtained 43 independent *L1OE* transgenic lines and 55 independent *L1^{A}OE* transgenic lines. All *L1OE* transgenics had similar morphologies to the wild-type, whereas *L1^{A}OE* transgenics showed dramatic morphological changes. We selected two representative transgenic lines from each group (*L1OE 9* and *L1OE 41* for *LTF1L1*-overexpression, and *L1^{A}OE 3* and *L1^{A}OE 24* for *LTF1L1^{A}*-overexpression) for further characterization (Fig. 6a).

Compared with the wild-type, *L1^{A}OE* plants exhibited an extremely dwarf phenotype with short plant height, internode length, diameters, and small leaves, whereas *L1OE* plants displayed no apparent morphological change except for *L1OE 41* plants, which were slightly shorter (Fig. 6a, Fig. S6). *LTF1L1* transcript levels in *L1OE* and *L1^{A}OE* transgenic plants were similar in different lines except for the *L1OE 41* (Fig. 6b). Further examination of LTF1L1 protein abundance revealed that the *L1^{A}OE* transgenic lines *L1^{A}OE 3*, *L1^{A}OE 24*, and the *L1OE* transgenic line *L1OE 9* accumulated similar levels of LTF1L1 protein, while the *L1OE* transgenic line *L1OE 41* accumulated a much higher level of LTF1L1 protein (Fig. 6c). Unlike LTF1 phosphorylation, which affects its protein stability in *Populus* (Gui et al., 2019), LTF1L1 phosphorylation did not affect its protein stability both in *Populus* and rice plants as the transcript and protein abundance of LTF1L1 was highly consistent (Fig. 4g,h, Fig. 6b,c). These results suggested that the different effects of protein phosphorylation between LTF1 and LTF1L1 are mainly due to their different sequences, not the different plant species.

To further examine the effects of *LTF1L1* and *LTF1L1^{A}* overexpression on lignin biosynthesis in *Populus*, we conducted histochemical staining followed by chemical tests and gene expression analysis. In *L1OE* plants, *L1OE 41* had less lignin in the wood cells, but *L1OE 9* did not show much difference from the wild-type (Fig. 6d). In *L1^{A}OE* plants, *L1^{A}OE 3* and *L1^{A}OE 24* had less lignin in the fiber cells and their xylem vessels were distorted or crushed (Fig. 6d). In agreement with this, lignin content was 18% lower in *L1OE 41*, 40% lower in *L1^{A}OE 3*, and 43% lower in *L1^{A}OE 24* than in the wild-type (Fig. 6e). Moreover, we measured the transcript levels of lignin biosynthesis genes (*PAL2*,

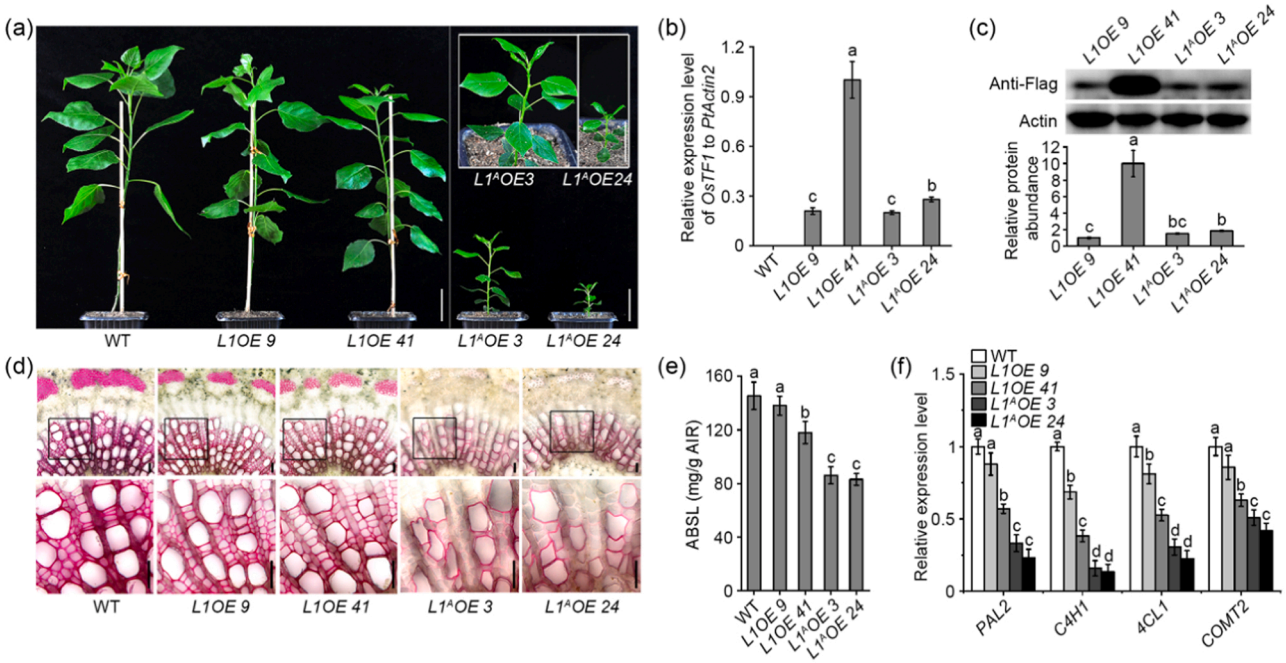

Fig. 6. Expression of *LTF1L1^{S169A}* in *Populus* suppressed lignin deposition by enhancing LTF1L1 repression activity, not stability. (a) Phenotypes of the WT, *LTF1L1* overexpressing (*L1OE*) and *LTF1L1^{A}* overexpressing (*L1^{A}OE*) transgenic *Populus* grown in phytotron at 2-month-old stage. Scale bar, 5 cm. **(b)** Relative expression level of *LTF1L1* in WT, *L1OE*, and *L1^{A}OE* transgenic lines at 2-month-old stage. Results are means ± SE of three biological repeats. **(c)** Protein abundance of LTF1L1 in WT, *L1OE*, and *L1^{A}OE* transgenic lines in *Populus* by immunoblotting assay (upper panel). The signal density was qualified based on the three biological replicates (lower panel). The relative protein abundance in *LTF1L1* overexpressing line *L1OE9* was set as 1. **(d)** Cross-sections of the 11th internode from WT, *L1OE*, and *L1^{A}OE* transgenics stained with phloroglucinol-HCl (upper panel). The lower panel shows close-up images of the lignified xylem cells (black box in the upper panel). Scale bar, 50 μm. **(e)** Lignin content in the stem xylem of WT, *L1OE*, and *L1^{A}OE* plants in *Populus* at 2-month-old stage. Results are means ± SE of three replicate determinations. **(f)** Expression of lignin biosynthesis genes in WT, *L1OE*, and *L1^{A}OE* transgenic lines at 2-month-old stage. Results are means ± SE of three biological repeats. In (b), (c), (e), and (f), different lowercase letters indicate significant differences at $P < 0.01$ by ANOVA.

C4H1, *4CL1*, and *COMT2* in *Populus*) in *L1OE* and *L1^{A}OE* transgenic plants. Like in rice, both *L1OE* and *L1^{A}OE* had lower gene expression than the wild-type, but *L1^{A}OE* had much lower gene expression than *L1OE* (Fig. 6f), which correlated with the lignin content in the different plants. These results suggested that the expression of non-phosphorylated LTF1L1 (LTF1L1^{S169A}) inhibits lignin biosynthesis by enhancing LTF1L1 transcriptional repressive ability, not by making it more stable, in both *Populus* and rice plants.

4. Discussion

In this study, we discovered a novel mechanism for regulating lignin biosynthesis in rice through protein phosphorylation. We showed that OsMPK6 phosphorylates LTF1L1 at Ser^{169} in the EAR motif, which reduces its transcriptional repression activity on lignin biosynthesis genes without affecting its protein stability. In contrast, non-phosphorylated LTF1L1 (LTF1L1^{A}) inhibits lignin biosynthesis by enhancing its transcriptional repression ability. Thus, the OsMPK6-LTF1L1 module dynamically modulates lignin biosynthesis in response to environmental stimuli (Fig. 7). This is different from the mechanism of *Populus* LTF1, which is degraded by PdMPK6-mediated phosphorylation (Gui et al., 2019).

4.1. The OsMPK6-LTF1L1 module: a novel mechanism controls lignin biosynthesis in rice

Lignin biosynthesis is a complex and dynamic process that depends on developmental and environmental cues (Gui et al., 2019). Different plants or cell types produce diverse lignin structures that have various functions (Boerjan et al., 2003; Vanholme et al., 2010; Dixon and Barros, 2019; Gui et al., 2020), but the molecular mechanisms that regulate them are still poorly understood. Protein phosphorylation is one of the potential mechanisms that modulate the activity, interaction, localization, or stability of lignin biosynthesis proteins (Zhang et al., 2018).

Previous studies have shown that MPK6 phosphorylates and degrades different MYB transcription factors that affect lignin biosynthesis in various plant species. For instance, in *Populus*, PdMPK6 targets LTF1 and degrades it by mechanical wounding, thereby relieving its negative effect on lignification (Gui et al., 2019). In Arabidopsis, MPK6 degrades MYB46 through the ubiquitin-proteasome pathway and reduces lignin biosynthesis under salt stress (Im et al., 2021). In rice, MPK6 participates in a MKP1-MPK3/6-MYB102 cascade that regulates vascular immunity and lignification in leaves (Lin et al., 2022). However, we discovered a novel mechanism in monocot rice, where OsMPK6 phosphorylates LTF1L1 at Ser^{169} and modulates its transcriptional repressive activity on lignin biosynthesis genes, without affecting its protein stability. We propose that the OsMPK6-LTF1L1 phosphorylation module is a unique way to fine-tune lignification in rice.

We also found that LTF1L1 is phosphorylated at Thr^{145} *in-vivo*, but not by OsMPK6, suggesting that another kinase is involved. It would be interesting to identify this kinase and its role in lignin biosynthesis. Moreover, future studies should uncover the signaling molecules and the upstream regulators of OsMPK6, as well as other lignin-related transcription factors that are phosphorylated by OsMPK6. These studies will help to elucidate the molecular mechanisms and the regulatory networks that govern lignin biosynthesis in a dynamic manner.

4.2. Phosphorylation of the EAR motif modulates MYB transcription factors activity

Lignin biosynthesis is controlled by a complex transcriptional network (Hirano et al., 2013b; Ye and Zhong, 2015). LTF1L1 is a rice R2R3-MYB factor thatrepresses lignin biosynthesis by directly binding to the promoter of *4CL3*, a key enzyme of monolignol biosynthesis (Gui et al., 2011). LTF1L1 function is modulated by its phosphorylation status, which is regulated by OsMPK6. This is similar to the finding that *Populus* LTF1 phosphorylation by PdMPK6 triggers its degradation and activates lignin biosynthesis in response to environmental stimuli (Gui et al., 2019). However, unlike *Populus* LTF1, LTF1L1 phosphorylation by OsMPK6 does not affect its protein stability, but rather modulates its transcriptional repressive activity on lignin biosynthesis (Fig. 7). Moreover, we identified Ser^{169} as the phosphorylation site of LTF1L1 by

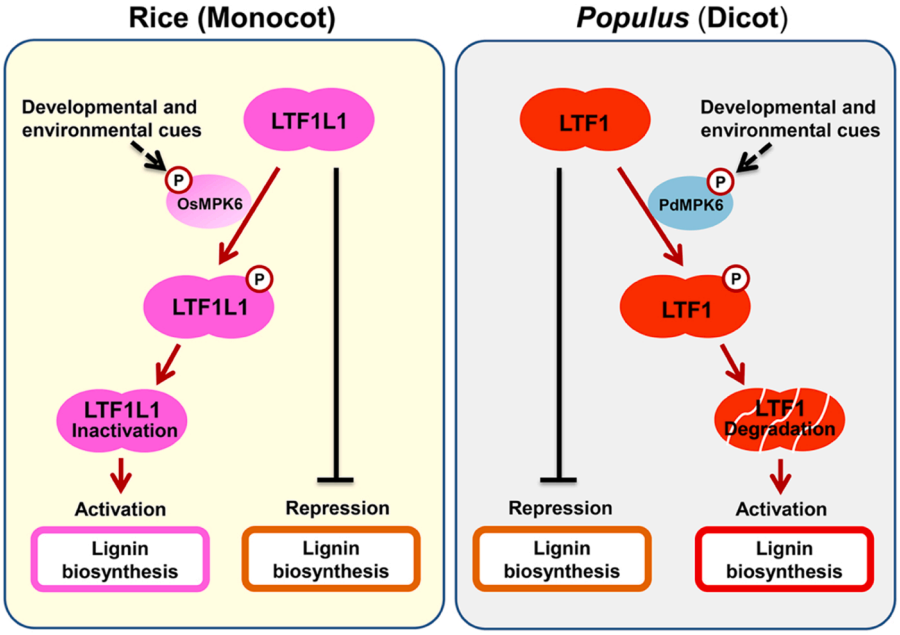

Fig. 7. Divergent roles of LTF1L1 and LTF1 phosphorylation by MPK6 in lignin biosynthesis in rice and *Populus*. LTF1L1 and LTF1 are homologous transcriptional repressors of lignin biosynthesis genes in rice and *Populus*, respectively. However, they are regulated differently by MPK6-mediated phosphorylation. In *Populus*, PdMPK6 phosphorylates LTF1, leading to its proteasome degradation and derepression of lignin biosynthesis (right panel) (Gui et al., 2019). In rice, OsMPK6 phosphorylates LTF1L1, which impairs its repressor activity but not its stability, allowing a flexible control of lignin biosynthesis in response to various cues (left panel).

OsMPK6, which is different from the phosphorylation sites of LTF1 (Thr^{146} and Thr^{178}) by PdMPK6 (Gui et al., 2019) (Fig. S7). These studies suggest that LTF1L1 and LTF1 have conserved roles in repressing lignin biosynthesis, but their functions are regulated by different mechanisms of protein phosphorylation in rice and *Populus*.

We also discovered a novel role of EAR motif phosphorylation in regulating transcriptional repressor activity. We showed that Ser^{169} which is located in the EAR motif of LTF1L1, is phosphorylated by OsMPK6 and reduces its transcriptional repressive activity on lignin biosynthesis genes (Fig. S7). The EAR motif enables the repressors to bind with corepressors and form a complex that acts as a negative regulator by altering the chromatin structure (Kagale and Rozwadowski, 2011; Oh et al., 2014). Mutations or modifications in the EAR motif may attenuate or eliminate the transcriptional repression of negative regulators (Zhang et al., 2013; Sun et al., 2023). Moreover, transcriptional activator can be changed to dominant repressors when they are fused to the EAR motif (Hiratsu et al., 2003). The phosphorylation sites in the EAR motif regions of IAA9, BEH4, and DEAR4 are conserved across evolutionarily diverse plant species, suggesting that these residues are possible regulators of protein functions (Kagale and Rozwadowski, 2011). Therefore, manipulating EAR motif phosphorylation may be an effective way to modulate lignin biosynthesis and other biological processes that are controlled by transcriptional repressors.

4.3. *Phosphorylation of MYB factors fine-tunes lignin biosynthesis by distinct mechanisms in rice and Populus*

Lignin biosynthesis is regulated by a complex transcriptional network that involves *MYB* factors. Our study demonstrated that MYB factors LTF1L1 and LTF1 are negative regulators of lignin biosynthesis in rice and *Populus*, respectively. LTF1L1 and LTF1 function are modulated by phosphorylation by MPK6 kinases, but the phosphorylation has differential effects on their stability and activity. Phosphorylation reduces the repressor activity of LTF1L1, while it triggers the degradation of LTF1 (Fig. 7). As a result, lignin biosynthesis genes are derepressed and lignin biosynthesis is activated in response to environmental stimuli. The different effects of phosphorylation are due to sequence divergence in the PEST motifs, the EAR motifs, and the phosphorylation sites of LTF1L1 and LTF1 (Fig. S7).

This study provides new insights into the molecular control of lignin formation and diversity in monocots and dicots, which are two major groups of angiosperms that diverged about 140–150 million years ago (Chaw et al., 2004). Monocots and dicots exhibit distinct growth patterns, adaptations, and lignin compositions. Dicots have lignin mainly composed of G and S units, while monocots have lignin with a significant amount of H units in addition to G and S units (Boerjan et al., 2003; Gui et al., 2020). This difference may reflect the divergent evolution of MYB genes that regulate lignin biosynthesis in these two groups. Our findings suggest potential strategies for engineering lignin biosynthesis in plants for biofuel and biomaterial applications by manipulating the phosphorylation status of the MYB factors.

CRediT authorship contribution statement

JSG, and LGL designed the research. JSG, PZ, YZ, LFL, JHS, JYS and LJC performed the research. JSG, LJC and LGL analyzed the data. JSG, LJC and LGL wrote the manuscript.

Declaration of Competing Interest

The authors declare that they have no known competing financial interests or personal relationships that could have appeared to influence the work reported in this paper. The authors declare no conflicts of interest.

Data availability

Data will be made available on request.

Acknowledgements

We thank Fan Chen (Institute of Genetics and Developmental Biology, Chinese Academy of Sciences) for providing the *dsg1* mutant; Wenli Hu for performing the GC–MS analysis; and Naixu Xu for help with the phosphorylation assay. This work was supported by the National Natural Science Foundation of China (31971617, 32022055), the Zhejiang A & F University Starting Funding (2021FR026), and the State Key Laboratory of Subtropical Silviculture (KF202002).

Appendix A. Supporting information

Supplementary data associated with this article can be found in the online version at doi:10.1016/j.plantsci.2023.111890.

References

E.G. Allwood, D.R. Davies, C. Gerrish, B.E. Ellis, G.P. Bolwell, Phosphorylation of phenylalanine ammonia-lyase: evidence for a novel protein kinase and identification of the phosphorylated residue, Febs Lett. 457 (1) (1999) 47–52.
W. Boerjan, J. Ralph, M. Baucher, Lignin biosynthesis, Annu. Rev. Plant Biol. 54 (2003) 519–546.
I. Cesarino, Structural features and regulation of lignin deposited upon biotic and abiotic stresses, Curr. Opin. Biotechnol. 56 (2019) 209–214.
S.M. Chaw, C.C. Chang, H.L. Chen, W.H. Li, Dating the monocot-dicot divergence and the origin of core eudicots using whole chloroplast genomes, J. Mol. Evol. 58 (4) (2004) 424–441.
Z. Chen, S. Teng, D. Liu, Y. Chang, L. Zhang, X. Cui, J. Wu, P. Ai, X. Sun, T. Lu, RLM1, encoding an R2R3 MYB transcription factor, regulates the development of secondary cell wall in rice, Front. Plant Sci. (2022) 13.
P. Cohen, The regulation of protein function by multisite phosphorylation–a 25 year update, Trends Biochem Sci. 25 (12) (2000) 596–601.
R.A. Dixon, J. Barros, Lignin biosynthesis: old roads revisited and new roads explored, Open Biol. 9 (12) (2019), 190215.
J. Gui, L. Luo, Y. Zhong, J. Sun, T. Umezawa, L. Li, Phosphorylation of LTF1, an MYB transcription factor in populus, acts as a sensory switch regulating lignin biosynthesis in wood cells, Mol. Plant 12 (10) (2019) 1325–1337.
J. Gui, J. Shen, L. Li, Functional characterization of evolutionarily divergent 4-coumarate:coenzyme a ligases in rice, Plant Physiol. 157 (2) (2011) 574–586.
J. Gui, S. Zheng, C. Liu, J. Shen, J. Li, L. Li, OsREM4. 1 interacts with OsSERK1 to coordinate the interlinking between abscisic acid and brassinosteroid signaling in rice, Dev. Cell 38 (2) (2016) 201–213.
J.S. Gui, P.Y. Lam, Y. Tobimatsu, J.Y. Sun, C. Huang, S.M. Cao, Y. Zhong, T. Umezawa, L. G. Li, Fibre-specific regulation of lignin biosynthesis improves biomass quality in Populus, N. Phytol. 226 (4) (2020) 1074–1087.
Y. Hiei, S. Ohta, T. Komari, T. Kumashiro, Efficient transformation of rice (Oryza sativa L.) mediated by Agrobacterium and sequence analysis of the boundaries of the T-DNA, Plant J. 6 (2) (1994) 271–282.
K. Hirano, K. Aya, Y. Morinaka, S. Nagamatsu, Y. Sato, B.A. Antonio, N. Namiki, Y. Nagamura, M. Matsuoka, Survey of genes involved in rice secondary cell wall formation through a co-expression network, Plant Cell Physiol. 54 (11) (2013a) 1803–1821.
K. Hirano, M. Kondo, K. Aya, A. Miyao, Y. Sato, B.A. Antonio, N. Namiki, Y. Nagamura, M. Matsuoka, Identification of transcription factors involved in rice secondary cell wall formation, Plant Cell Physiol. 54 (11) (2013b) 1791–1802.
K. Hiratsu, K. Matsui, T. Koyama, M. Ohme-Takagi, Dominant repression of target genes by chimeric repressors that include the EAR motif, a repression domain, in Arabidopsis, Plant J. 34 (5) (2003) 733–739.
J.H. Im, J.H. Ko, W.C. Kim, B. Crain, D. Keathley, K.H. Han, Mitogen-activated protein kinase 6 negatively regulates secondary wall biosynthesis by modulating MYB46 protein stability in Arabidopsis thaliana, PLoS Genet 17 (4) (2021), e1009510.
S. Kagale, K. Rozwadowski, EAR motif-mediated transcriptional repression in plants: an underlying mechanism for epigenetic regulation of gene expression, Epigenetics 6 (2) (2011) 141–146.
M. Kishi-Kaboshi, K. Okada, L. Kurimoto, S. Murakami, T. Umezawa, N. Shibuya, H. Yamane, A. Miyao, H. Takatsuji, A. Takahashi, A rice fungal MAMP-responsive MAPK cascade regulates metabolic flow to antimicrobial metabolite synthesis, Plant J. 63 (4) (2010) 599–612.
W. Lan, F. Lu, M. Regner, Y. Zhu, J. Rencoret, S.A. Ralph, U.I. Zakai, K. Morreel, W. Boerjan, J. Ralph, Tricin, a flavonoid monomer in monocot lignification, Plant Physiol. 167 (4) (2015) 1284–1295.
L. Li, Y. Zhou, X. Cheng, J. Sun, J.M. Marita, J. Ralph, V.L. Chiang, Combinatorial modification of multiple lignin traits in trees through multigene cotransformation, Proc. Natl. Acad. Sci. 100 (8) (2003) 4939–4944.

H. Lin, M. Wang, Y. Chen, K. Nomura, S. Hui, J. Gui, X. Zhang, Y. Wu, J. Liu, Q. Li, An MKP-MAPK protein phosphorylation cascade controls vascular immunity in plants, Sci. Adv. 8 (10) (2022) eabg8723.
C. Liu, H. Yu, X. Rao, L. Li, R.A. Dixon, Abscisic acid regulates secondary cell-wall formation and lignin deposition in Arabidopsis thaliana through phosphorylation of NST1, Proc. Natl. Acad. Sci. 118 (5) (2021), e2010911118.
S. Liu, L. Hua, S. Dong, H. Chen, X. Zhu, J. Jiang, F. Zhang, Y. Li, X. Fang, F. Chen, OsMAPK6, a mitogen-activated protein kinase, influences rice grain size and biomass production, Plant J. 84 (4) (2015) 672–681.
Y. Liu, E. Leary, O. Saffaf, R. Frank Baker, S. Zhang, Overlapping functions of YDA and MAPKKK3/MAPKKK5 upstream of MPK3/MPK6 in plant immunity and growth/development, J. Integr. Plant Biol. 64 (8) (2022) 1531–1542.
L. Luo, L. Li, Molecular understanding of wood formation in trees, For. Res. 2 (1) (2022), 0-0.
D. Ma, C.P. Constabel, MYB repressors as regulators of phenylpropanoid metabolism in plants, Trends Plant Sci. 24 (3) (2019) 275–289.
X. Ma, Q. Zhang, Q. Zhu, W. Liu, Y. Chen, R. Qiu, B. Wang, Z. Yang, H. Li, Y. Lin, A robust CRISPR/Cas9 system for convenient, high-efficiency multiplex genome editing in monocot and dicot plants, Mol. Plant 8 (8) (2015) 1274–1284.
T. Miyamoto, R. Takada, Y. Tobimatsu, Y. Takeda, S. Suzuki, M. Yamamura, K. Osakabe, Y. Osakabe, M. Sakamoto, T. Umezawa, Os MYB 108 loss-of-function enriches p-coumaroylated and tricin lignin units in rice cell walls, Plant J. 98 (6) (2019) 975–987.
S. Noda, T. Koshiba, T. Hattori, M. Yamaguchi, S. Suzuki, T. Umezawa, The expression of a rice secondary wall-specific cellulose synthase gene, OsCesA7, is directly regulated by a rice transcription factor, OsMYB58/63, Planta 242 (2015) 589–600.
E. Oh, J.-Y. Zhu, H. Ryu, I. Hwang, Z.-Y. Wang, TOPLESS mediates brassinosteroid-induced transcriptional repression through interaction with BZR1, Nat. Commun. 5 (1) (2014) 4140.
D. Ohman, B. Demedts, M. Kumar, L. Gerber, A. Gorzsas, G. Goeminne, M. Hedenstrom, B. Ellis, W. Boerjan, B. Sundberg, MYB103 is required for FERULATE-5-HYDROXYLASE expression and syringyl lignin biosynthesis in Arabidopsis stems, Plant J. 73 (1) (2013) 63–76.
F.A. Pettolino, C. Walsh, G.B. Fincher, A. Bacic, Determining the polysaccharide composition of plant cell walls, Nat. Protoc. 7 (9) (2012) 1590–1607.
A.L. Schilmiller, J. Stout, J.K. Weng, J. Humphreys, M.O. Ruegger, C. Chapple, Mutations in the cinnamate 4–hydroxylase gene impact metabolism, growth and development in Arabidopsis, Plant J. 60 (5) (2009) 771–782.
D.B. Sulis, J.P. Wang, Regulation of lignin biosynthesis by post-translational protein modifications, Front. Plant Sci. 11 (2020) 914.
H. Sun, K. Hu, S. Wei, G. Yao, H. Zhang, Ethylene response factors 4.1/4.2 with an EAR motif repress anthocyanin biosynthesis in red-skinned pears, Plant Physiol.: kiad0 (2023) 68..
T. Sun, Y. Nitta, Q. Zhang, D. Wu, H. Tian, J.S. Lee, Y. Zhang, Antagonistic interactions between two MAP kinase cascades in plant development and immune signaling, EMBO Rep. 19 (7) (2018), e45324.
R. Vanholme, B. Demedts, K. Morreel, J. Ralph, W. Boerjan, Lignin biosynthesis and structure, Plant Physiol. 153 (3) (2010) 895–905.
I.-C. Vélez-Bermúdez, J.E. Salazar-Henao, S. Fornalé, I. López-Vidriero, J.-M. Franco-Zorrilla, E. Grotewold, J. Gray, R. Solano, W. Schmidt, M. Pagés, A MYB/ZML complex regulates wound-induced lignin genes in maize, Plant Cell 27 (11) (2015) 3245–3259.
S.R. Verma, U. Dwivedi, Lignin genetic engineering for improvement of wood quality: applications in paper and textile industries, fodder and bioenergy production, South Afr. J. Bot. 91 (2014) 107–125.
H. Wang, Q. Zhao, F. Chen, M. Wang, R.A. Dixon, NAC domain function and transcriptional control of a secondary cell wall master switch, Plant J. 68 (6) (2011) 1104–1114.
J.P. Wang, L. Chuang, P.L. Loziuk, H. Chen, Y.-C. Lin, R. Shi, G.-Z. Qu, D.C. Muddiman, R.R. Sederoff, V.L. Chiang, Phosphorylation is an on/off switch for 5-hydroxyconiferaldehyde O-methyltransferase activity in poplar monolignol biosynthesis, Proc. Natl. Acad. Sci. 112 (27) (2015) 8481–8486.
L. Wu, M. Zhang, R. Zhang, H. Yu, H. Wang, J. Li, Y. Wang, Z. Hu, Y. Wang, Z. Luo, et al., Down-regulation of OsMYB103L distinctively alters beta-1,4-glucan polymerization and cellulose microfibers assembly for enhanced biomass enzymatic saccharification in rice, Biotechnol. Biofuels 14 (1) (2021) 245.
M. Xie, J. Zhang, T.J. Tschaplinski, G.A. Tuskan, J.G. Chen, W. Muchero, Regulation of lignin biosynthesis and its role in growth-defense tradeoffs, Front Plant Sci. 9 (2018) 1427.
C. Yang, D. Li, X. Liu, C. Ji, L. Hao, X. Zhao, X. Li, C. Chen, Z. Cheng, L. Zhu, OsMYB103L, an R2R3-MYB transcription factor, influences leaf rolling and mechanical strength in rice (Oryza sativa L.), BMC Plant Biol. 14 (2014) 158.
Y. Ye, B. Liu, M. Zhao, K. Wu, W. Cheng, X. Chen, Q. Liu, Z. Liu, X. Fu, Y. Wu, CEF1/OsMYB103L is involved in GA-mediated regulation of secondary wall biosynthesis in rice, Plant Mol. Biol. 89 (4–5) (2015) 385–401.
Z.H. Ye, R. Zhong, Molecular control of wood formation in trees, J. Exp. Bot. 66 (14) (2015) 4119–4131.
S.-D. Yoo, Y.-H. Cho, J. Sheen, Arabidopsis mesophyll protoplasts: a versatile cell system for transient gene expression analysis, Nat. Protoc. 2 (7) (2007) 1565–1572.
K. Yoshida, S. Sakamoto, T. Kawai, Y. Kobayashi, K. Sato, Y. Ichinose, K. Yaoi, M. Akiyoshi-Endo, H. Sato, T. Takamizo, Engineering the Oryza sativa cell wall with rice NAC transcription factors regulating secondary wall formation, Front. Plant Sci. 4 (2013) 383.
H. Zhang, J. Zhang, R. Quan, X. Pan, L. Wan, R. Huang, EAR motif mutation of rice OsERF3 alters the regulation of ethylene biosynthesis and drought tolerance, Planta 237 (2013) 1443–1451.
M. Zhang, J. Su, Y. Zhang, J. Xu, S. Zhang, Conveying endogenous and exogenous signals: MAPK cascades in plant growth and defense, Curr. Opin. Plant Biol. 45(Pt A) (2018) 1–10.
C. Zhao, P. Wang, T. Si, C.C. Hsu, L. Wang, O. Zayed, Z. Yu, Y. Zhu, J. Dong, W.A. Tao, et al., MAP kinase cascades regulate the cold response by modulating ICE1 protein stability, Dev. Cell 43 (5) (2017), 618-629 e615.
R. Zhong, C. Lee, R.L. McCarthy, C.K. Reeves, E.G. Jones, Z.H. Ye, Transcriptional activation of secondary wall biosynthesis by rice and maize NAC and MYB transcription factors, Plant Cell Physiol. 52 (10) (2011) 1856–1871.
J. Zhou, C. Lee, R. Zhong, Z.-H. Ye, MYB58 and MYB63 are transcriptional activators of the lignin biosynthetic pathway during secondary cell wall formation in Arabidopsis, Plant Cell 21 (1) (2009) 248–266.
M. Zhou, K. Zhang, Z. Sun, M. Yan, C. Chen, X. Zhang, Y. Tang, Y. Wu, LNK1 and LNK2 corepressors interact with the MYB3 transcription factor in phenylpropanoid biosynthesis, Plant Physiol. 174 (3) (2017) 1348–1358.